

Di-Hydroxylated Soybean Oil Polyols with Varied Hydroxyl Values and Their Influence on UV-Curable Pressure-Sensitive Adhesives

Yonghui Li · Xiuzhi Susan Sun

Received: 6 February 2014 / Revised: 27 March 2014 / Accepted: 8 April 2014 / Published online: 27 April 2014
© AOCS 2014

Abstract Di-hydroxylated soybean oil (DSO) polyols with three different hydroxyl values (OHV) of 160, 240, and 285 mg KOH/g were synthesized from epoxidized soybean oils (ESO) by oxirane cleavage with water catalyzed by perchloric acid. The DSO were clear, viscous liquids at room temperature. The structure and physical properties of DSO were characterized using titration methods, Fourier-transform infrared spectroscopy (FTIR), gel permeation chromatography, rheometer, differential scanning calorimetry, and thermogravimetric analysis. The number average molecular weight of DSO160, DSO240, and DSO285 were 1,412, 1,781, and 1,899 g/mol, respectively, indicating that oligomerization occurred during DSO synthesis, which was further confirmed by FTIR. All DSO polyols exhibited non-Newtonian, shear thinning behavior. DSO with higher OHV were more viscous than those with lower OHV. All DSO were thermally stable up to 380 °C. These three DSO were formulated into pressure-sensitive adhesives (PSA) by copolymerizing with ESO using UV curing. The peel adhesion strength of the PSA was significantly affected by the OHV of DSO and DSO content. Maximal PSA adhesion strength of 4.6 N/inch was obtained with DSO285 and a DSO/ESO weight ratio of 0.75.

Keywords Epoxidized soybean oil(s) (ESO) · Di-hydroxylated soybean oil · Polyol · Hydroxyl value(s) (OHV) · Physical properties · UV-curing · Pressure-sensitive adhesive(s) (PSA) · Peel adhesion strength · Biobased product

Introduction

Pressure-sensitive adhesives (PSA) have been widely used in many fields as tapes, labels, protection films, etc. Current PSA are made predominately from petrochemicals, such as acrylics, silicones, synthetic polyisoprene, polybutadienes, and various copolymers [1]. Developing PSA resins from renewable bio-resources is economically attractive and socially responsible [2–6].

Vegetable oils from oilseeds such as soybean, palm, rapeseed, canola, and camelina mainly contain triglycerides molecules in which the three hydroxyl functions of glycerin are esterified with fatty acids. These fatty acids could be saturated, with non-reactive aliphatic chains, or unsaturated, with aliphatic chains bearing double bonds. Direct polymerization of unsaturated oils is rarely successful due to the presence of allyl hydrogens, except for some oils such as tung oil, which has conjugated double bonds [7]. These unsaturated oils could provide a solid platform for further modifications into oil derivatives, and various oil derived resins and polymers have been reported, e.g., epoxides, polyols, acrylates, polyacids, polyamines, polyurethanes, etc. [4, 8–12]. Among various vegetable oils, soybean oil is one of the most attractive types for large-scale industrial products due to its abundance and high degree of unsaturation [13].

Soybean oil polyols are usually produced by the epoxidation of double bond sites, followed by oxirane ring opening with proton donors. Oils are typically epoxidized by generating a peracid in situ from hydrogen peroxide and acetic or formic acid [11]. Many types of proton donors have been used to ring-open the epoxide for polyols, such as methanol, hydrochloric acid, hydrobromic acid, hydrogen, etc. [8, 14–18]. Most of these polyols are developed mainly for the purpose of polyurethane synthesis [7, 11,

Y. Li · X. S. Sun (✉)
Bio-Materials and Technology Lab, Department of Grain
Science and Industry, Kansas State University, Manhattan,
KS 66506, USA
e-mail: xss@ksu.edu

13]. Researchers have found that the higher the hydroxyl functionality of the polyols, the higher the glass transition temperature and crosslinking density of the polyurethane network [19]; therefore, the functionality of soybean polyols is closely related to polymer performance. The hydroxyl functionality of soybean polyols generated from the above methods is relatively low, which limits their application in PSA.

Sun and co-workers previously developed soybean polyols with higher hydroxyl functionality to provide the reactive functional groups and adequate adhesivity to formulate PSA resins from soybean oils. Each oxirane group was converted into two hydroxyl groups, namely dihydroxylated soybean oil (DSO), by using water as a proton donor to ring-open the oxirane of epoxidized soybean oil (ESO) [6, 20]. Each soybean triglyceride theoretically contains an average of 4.6 double bonds [13], corresponding to a maximal hydroxyl functionality of 9.2 and hydroxyl value (OHV) of 498 mg KOH/g. Because of the incomplete conversion of the double bond to oxirane and the oligomerization reaction during the hydroxylation of oxirane with water catalyzed by strong acid, however, the maximum OHV of DSO obtained with this approach was around 290 mg KOH/g [20]. To determine the effects of DSO OHV on PSA performance, in this work, DSO with varied OHV were synthesized by controlling the reaction conditions, then characterized for physical and chemical properties and evaluated for PSA performance.

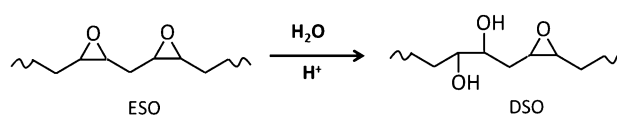
Experimental Procedures

Materials

ESO (VIKOFLEX[®]7170) was provided by Arkema Inc. PC-2506 (diaryliodonium hexafluoroantimonate) was used as a cationic photo initiator and obtained from the Polyset Company. Rosin ester was from Arizona Chemical. Perchloric acid (70 % solution in water) and other chemicals were purchased from Fisher Scientific.

Synthesis of DSO

DSO synthesis was carried out in a 250-mL Erlenmeyer flask equipped with a magnetic stirrer. For a typical reaction, 70 g ESO was placed in the flask, and 70 mL tetrahydrofuran (THF) was added to dissolve the ESO. Then, 35 mL of distilled water and a determined amount of perchloric acid were mixed in another container and dropped into the flask gradually (within 2 min) while stirring. The reaction was continued for a preset time at room temperature. Perchloric acid content and reaction time were varied so that DSO with different OHV can be



Scheme 1 Chemical pathways of DSO polyols synthesis with varied hydroxyl values from ESO

obtained (Scheme 1). DSO 160 was synthesized with 1 % (v/w, based on ESO) perchloric acid for 80 min; DSO240 was also synthesized with 1 % acid, but for 150 min; and DSO 285 was synthesized with 1.5 % acid for 300 min. At the end of the reaction, the sample was immediately extracted with ethyl acetate in a separating funnel, washed with distilled water, neutralized with saturated sodium bicarbonate solution, and finally evaporated using a rotary evaporator first under low vacuum (~ 100 Torr) for 1 h, then under high vacuum (~ 0.1 Torr) for an additional 2 h at 80 °C to remove solvent and water. The sample was collected and stored at room temperature for future measurements.

Physical Attributes of DSO

The residue oxirane oxygen content in DSO was measured according to ASTM D 1652-97 (Test Method A). The hydroxyl value (OHV) of DSO was measured according to ASTM D 4274-99 (Test Method A-Acetylation). The water content of DSO was measured using Karl Fischer titration with a Mettler-Toledo V30 Titrator.

The molecular weight was determined by gel permeation chromatography (GPC) (Waters 2695 Separation Module pump and Waters 2414 Differential Refractometer/2998 Photodiode Array Detector) with Viscotek I-MBHMW and I-MBLMW columns. The measurement was taken at room temperature using dimethylformamide as the eluent with a flow rate of 1 ml/min and an injection volume of 100 μ L. The molecular weight was calibrated according to the polystyrene standard.

Fourier-Transform Infrared (FTIR) Spectroscopy of DSO

FTIR spectra were acquired with a Perkin Elmer Spectrum 400 FT-IR/FT-NIR Spectrometer (Waltham, MA, USA). Spectra were collected in the region of 4,000–400 cm^{-1} with a spectral resolution of 4 cm^{-1} and 32 scans co-added.

Rheology of DSO

The rheological properties of ESO and DSO were measured with a Bohlin CVOR 150 rheometer (Malvern Instruments, Southborough, MA, USA) with a PP 20

parallel plate with gap size of 1,000 μm . Two different rheological studies were conducted on each sample type. The rate sweep was carried out with shear rates ranging from 0.01 to 100 s^{-1} at 25 $^{\circ}\text{C}$. The temperature sweep was conducted with temperatures ranging from 20 to 90 $^{\circ}\text{C}$, with a heating rate of 5 $^{\circ}\text{C}/\text{min}$ and a fixed shear rate of 10 s^{-1} . Viscosity as a function of shear rate and temperature was recorded.

Differential Scanning Calorimetry (DSC) of DSO

Thermal transitions of ESO and DSO were measured with a TA DSC Q200 instrument in an inert environment using nitrogen with a gas flow rate of 50 ml/min. A sample of about 10 mg of oil was sealed in a stainless steel pan. An empty pan was used as a reference. The sample was heated from -90 to 100 $^{\circ}\text{C}$ at a rate of 10 $^{\circ}\text{C}/\text{min}$. Phase transition temperatures, including glass transition (T_g), cold crystallization (T_c), and melting (T_m), and heat capacity (ΔC_p), heat of cold crystallization (ΔH_c), and heat of melting (ΔH_m) were obtained.

Thermogravimetric Analysis (TGA) of DSO

Thermal stability of DSO was determined with a Perkin Elmer Pyris1 TGA instrument. A sample of about 10 mg was placed in a platinum TGA pan and heated from 50 $^{\circ}\text{C}$ to 600 $^{\circ}\text{C}$ at a heating rate of 20 $^{\circ}\text{C}/\text{min}$ under a nitrogen atmosphere. The thermal decomposition temperatures $T_{d,10\%}$ (temperature at 10 % weight loss) and $T_{d,max}$ (temperature at maximum decomposition rate) were recorded.

PSA Preparation and Peel Adhesion Test

We prepared a series of PSA samples to study the effect of DSO concentrations and OHV on PSA performance. Rosin ester as a common tackifier was added to the resin formulation to improve the adhesion and tackiness of the PSA [6]. The DSO/ESO ratio of each DSO type varied, whereas the rosin ester/ESO ratio (0.7, w/w) and photo initiator/ESO ratio (3 %, w/w) remained constant throughout the experiments. For a typical process, determined amounts of ESO, DSO, rosin ester, and photo initiator were weighed and transferred into a 25-mL glass vial to form adhesion resin. The vial was sealed and placed into a sonicator filled with heated water (~ 70 $^{\circ}\text{C}$). A heat gun and Vortex mixer were also used to help melt rosin ester and mix the material. The mixing step was completed when photo initiator particles could not be observed by naked eyes. The adhesive mixture was coated onto PET film using a EC-200 Drawdown Coater with #6

wire rod (Chem Instruments) to obtain PSA coatings. The coating amount was calculated to be 14.58 g/m^2 . The PSA coatings were cured by a Fusion 300S 6-in. UV system (300 W/inch power, D bulb, UV radiation does 215–231 mJ/cm^2) equipped with an LC6B bench-top conveyor to obtain PSA tape samples. The irradiation ranged from 200 to 600 nm, with significant enhancement in 350–400 nm. The conveyor speed was set at 7 ft/min. The number of UV passes to completely cure the PSA coatings was recorded.

The PSA tapes were then cut into 1-in. \times 5-in. stripes. The peel adhesion strength was measured following ASTM D3330/D3330 M-04 (2010). At least three specimens were measured for each type of PSA.

Photocalorimetry-DSC

The photocalorimetric measurements of PSA resins were performed with a TA Q200 DSC coupled to a photocalorimeter accessory (PCA, OmniCure S2000, TA instruments) equipped with a high-pressure 200-W mercury lamp. The UV wavelength was adjusted to 320–500 nm using a cut-off filter, and light intensity of 100 mW/cm^2 was used. Approximately 5 mg of each resin was accurately weighed in an open aluminum pan, and an empty aluminum pan was used as reference. The sample was equilibrated at 25 $^{\circ}\text{C}$ for 0.5 min without UV, then UV-irradiated for 15 min under a nitrogen atmosphere. The 15 min of exposure was sufficient to completely cure the resin. The peak time (time at peak subtracted by the equilibration time of 0.5 min) was recorded to characterize the curing speed of each resin. Regular DSC was also conducted to evaluate the glass transition temperatures of UV-cured PSA.

Results and Discussion

Epoxy Oxygen Content and Hydroxyl Value

The three DSO polyols appeared as clear liquids with almost no color at room temperature. The epoxy oxygen content of ESO was measured as 6.68 %, which is slightly lower than the company-reported value of 7.0 %. By oxygen cleavage conversion of ESO to DSO, the epoxy oxygen content decreased, whereas OHV increased (Table 1). DSO160 has an epoxy oxygen content of 3.59 % and OHV of 157.2 mg KOH/g, showing that over half of the oxirane has been cleaved and DSO160 possesses both oxirane and hydroxyl functional groups. DSO240 had an epoxy oxygen content of 0.82 % and OHV of 238.7 mg KOH/g. The oxirane in DSO285 was almost completely

Table 1 Physical properties of DSO

Sample ID	Epoxy oxygen (%)	OHV (mg KOH/g)	Mn, Mw (g/mol)	f_{Ep} , e_{qEp} /mol	f_{OH} , e_{qOH} /mol	Water content (% w/w)	Viscosity ^a (Pa·s)
ESO	6.68 ± 0.04	/	1006,1291	4.3 ± 0.03	0	0.20	0.47 ± 0.07
DSO160	3.59 ± 0.02	157.2 ± 7.1	1412,2106	3.2 ± 0.02	4.0 ± 0.2	0.46	2.53 ± 0.22
DSO240	0.82 ± 0.07	238.7 ± 2.9	1781,2522	0.9 ± 0.08	7.6 ± 0.1	0.55	25.45 ± 1.77
DSO285	0.17 ± 0.03	284.2 ± 1.5	1899,2656	0.2 ± 0.03	9.6 ± 0.1	0.47	44.29 ± 2.72

f_{Ep} epoxide functionality, f_{OH} hydroxyl functionality

^a Viscosity values shown here were obtained at 25 °C with a shear rate of 10 s⁻¹

converted, with oxirane oxygen residue of only 0.17 % and OHV of 284.2 mg KOH/g.

Average oxirane group functionality (f_{Ep}) of ESO and DSO was calculated according to Eq. (1) below and is listed in Table 1:

Average oxirane functionality:

$$f_{Ep} = \frac{\text{Oxirane oxygen \%} \times \text{Number average molecular weight}}{16} \quad (1)$$

The measured Mn of ESO was 1,006 g/mol. ESO was calculated as possessing 4.3 oxirane groups per triglyceride (f_{Ep} , slightly lower than the theoretical oxirane groups of 4.6 due to incomplete conversion or side reactions during epoxidation). If all the ESO oxirane groups were converted into di-hydroxyl groups, DSO should have an OHV of 482 mg KOH/g. In reality, the maximum OHV of DSO we were able to obtain was about 290 mg KOH/g. This was caused by considerable oligomerization during DSO synthesis, which occurred between oxirane–oxirane, oxirane–hydroxyl, or hydroxyl–hydroxyl groups catalyzed by acid. Oligomerization is a common side reaction during hydroxylation of epoxidized oils with ring opening agents, as reported previously [21, 22]. The oligomerization in this study was evidenced by the obviously increase in molecular weights of DSO compared with that of ESO (Table 1). The number-average molecular weight (Mn) and weight-average molecular weight (Mw) of DSO160, DSO240, and DSO285 were 1,412/2,106, 1,781/2,522, and 1,899/2,656 g/mol, respectively. The oligomerization is further supported by the presence of an ether group band in FTIR spectra, which is discussed in the next section. The average OH functionality (f_{OH}) of the three DSO was calculated according to Eq. (2) below, and values are listed in Table 1:

Average OH functionality:

$$f_{OH} = \frac{\text{OHV} \times \text{Number average molecular weight}}{56100} \quad (2)$$

Water content of DSO was determined by Karl Fischer titration method, and the values were around 0.5 %.

FTIR

The functional groups of ESO and DSO were observed (Fig. 1a): they include: O–H (~ 3,400 cm⁻¹), alkyl C–H (2,920, 2,860, 1,460, 1,380, and 726 cm⁻¹), ester C=O (1,740, 1,240, and 1,160 cm⁻¹), epoxy group (822 and 842 cm⁻¹), and ether group (1,067 cm⁻¹). Compared to the spectrum of ESO, the intensity of epoxy group bands was significantly reduced in DSO (Fig. 1c, enlarged area), whereas the intensity of OH group bands was obviously enhanced (Fig. 1b, enlarged area). The epoxy group bands disappeared completely for DSO285, and the intensity of the OH band for DSO285 reached a maximum compared with DSO160 and DSO240, which was consistent with the trend of epoxy oxygen content and OHV as shown in Table 1. The appearance of the ether group in DSO240 and DSO285 was attributed to oligomerization, as discussed in the previous section.

Rheological Properties

Both ESO and DSO polyols exhibited obviously non-Newtonian, shear-thinning behavior (Fig. 2a). For example, the viscosity of DSO285 was observed to drop from approximately 1.6 × 10⁵ cP at a shear rate of 0.01 s⁻¹ to 4.4 × 10⁴ cP at a shear rate of 1 s⁻¹; the viscosity of ESO was observed to drop from approximately 7.8 × 10³ cP at a shear rate of 0.01 s⁻¹ to 4.2 × 10² cP at a shear rate of 1 s⁻¹. At a shear rate above 1 s⁻¹, the viscosity was more independent of shear rate. The viscosity values at the shear rate of 10 s⁻¹ are summarized in Table 1. ESO obviously has the lowest viscosity, which increases as OHV increases, resulted from the increase in polarity and molecular weight. More hydroxyl groups increased the polarity of DSO molecule, leading to a higher resistance to flow, thus higher viscosity. Furthermore, the molecular weight increased as DSO OHV increased (Table 1), which also led to increased viscosity.

The DSO polyols are very temperature-sensitive (Fig. 2b). The viscosity of DSO decreased greatly as temperature increased, then slowly to almost stable

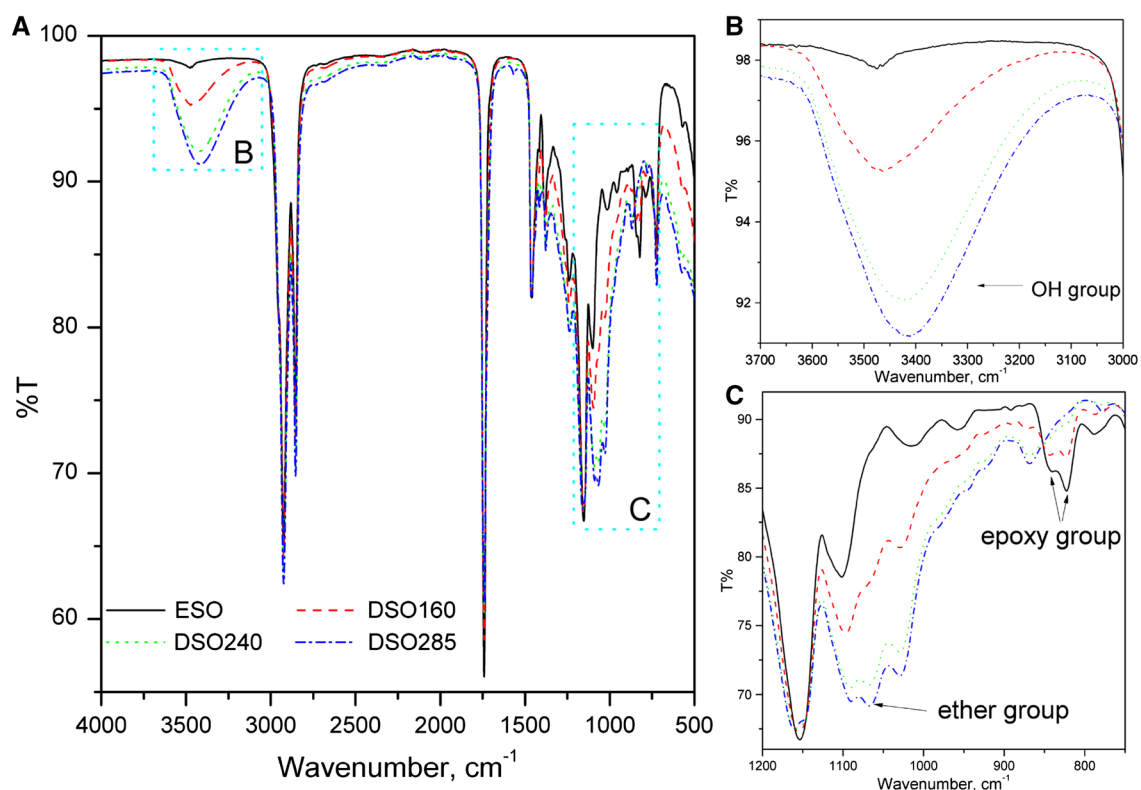


Fig. 1 FTIR spectra of ESO and DSO (b and c area in a are enlarged at right)

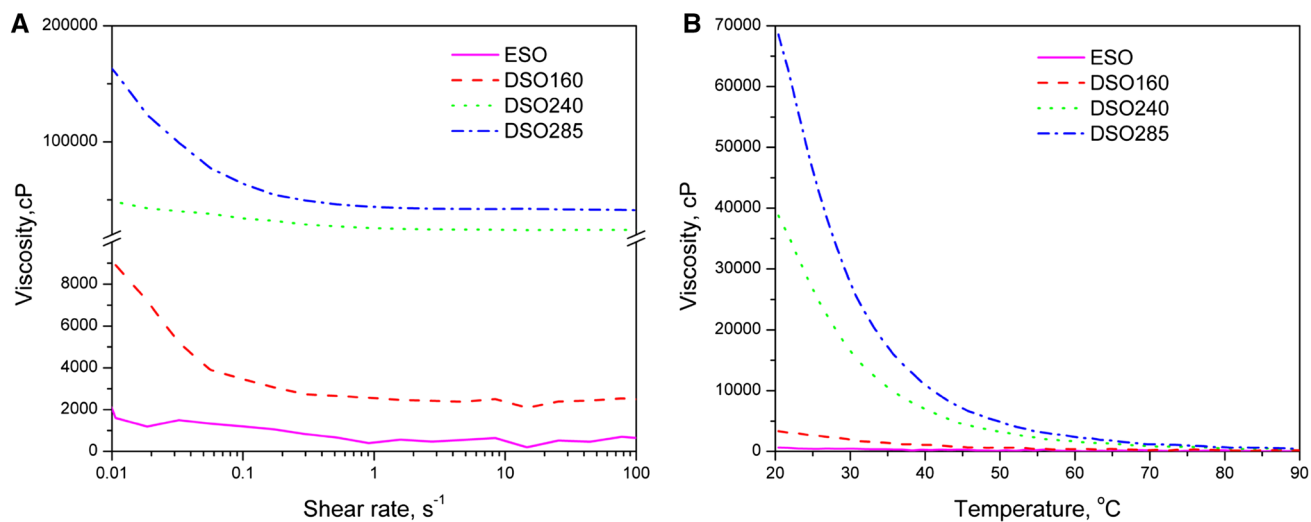


Fig. 2 Effect of shear rate (a) and temperature (b) on the viscosity of ESO and three DSO

above 70 °C. For example, the viscosity of DSO285 dropped from 6.9×10^4 cP at 20 °C to 1.2×10^3 cP at 70 °C, and the viscosity of DSO240 dropped from 3.9×10^4 cP at 20 °C to 8.6×10^2 cP at 70 °C. Reduced viscosity at elevated temperatures helps dissolve and thoroughly mix DSO with other PSA components.

Thermal Properties

Both ESO and DSO are liquid at room temperature. Glass transition, crystallization, and melting point all occurred below room temperature (Fig. 3; Table 2). ESO had a T_g of -63.7 °C, T_c of -28.1 °C, and double melting peaks at -13.9 °C and -5.5 °C. The T_g of DSO increased as the

DSO OHV increased; for e.g., the T_g of DSO160 was -48.4 °C, whereas that of DSO285 was -22.8 °C. The increased T_g might be explained by both enhanced hydrogen bonding and the larger molecular weight of DSO with high OHV. T_c of DSO240 and DSO285 was observed at -10.86 and -5.6 °C, respectively, but we did not notice an obvious cold crystallization peak of DSO160. DSO160 also exhibited double melting peaks at -0.2 and 12.2 °C, which were larger than for ESO, but smaller than those of DSO240 and DSO285. T_m of DSO240 and DSO285 was 17.2 and 18.1 °C, respectively. All oil samples were thermally stable until around 380 °C (Fig. 4; Table 2). The observed thermal behavior differences of samples were caused by their different structures.

Peel Adhesion Strength of PSA from ESO and DSO Polyols

PSAs from ESO and DSO with various OHVs were prepared to study the effect of DSO concentration and OHV on the curing speed and peel adhesion strength (Table 3). The number of UV passes was used to

illustrate the curing speed of PSA resin; a larger number of UV passes indicates a slower curing speed of the PSA resin. ESO alone was cured with only one UV pass. The curing speed of PSA samples with DSO160 decreased as DSO content increased. A similar phenomenon was also observed with DSO240 and DSO285. We further found that the curing speed was affected by not only DSO content, but also the OHV of DSO; for example, the PSA resin formulated with DSO285 at 1:1 DSO/ESO (w/w) (DSO285-1) was not completely cured even after 42 UV passes. We calculated the mole ratio of hydroxyl group to epoxy group (n_{OH}/n_{Ep}) in each formulation and noticed that the larger the value of n_{OH}/n_{Ep} in the resin, the longer it takes to cure. The UV-curing process of PSA resins containing both ESO and DSO involves two distinct reactions: one is the homopolymerization of epoxy groups, and the other is the copolymerization of epoxy groups and hydroxyl groups, although both reactions resulted in the formation of ether linkages (Scheme 2). If there are excessive hydroxyl groups compared with epoxy groups in the resin, it may not be curable, as was the case with DSO285-1.

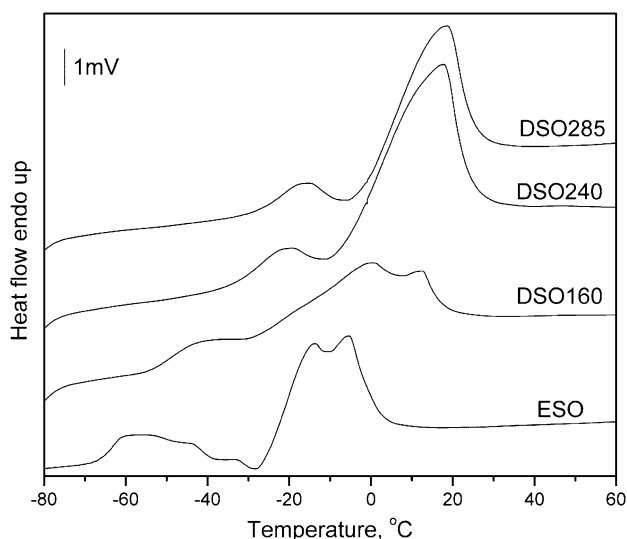


Fig. 3 DSC thermograms of ESO and DSO with various OHV

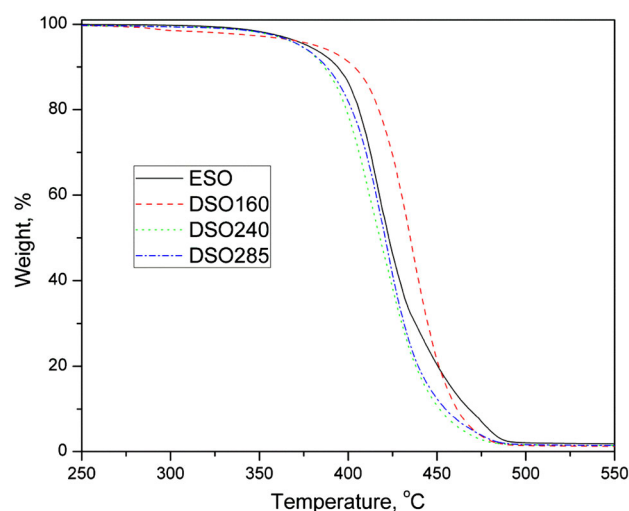


Fig. 4 TGA thermograms of ESO and DSO with various OHV

Table 2 Thermal properties of ESO and DSO polyols

Sample ID	T_g (°C)	ΔC_p (J/(g°C))	T_c (°C)	ΔH_c (J/g)	T_m (°C)	ΔH_m (J/g)	$T_{d,10}$ % (°C)	$T_{d,max}$ (°C)
ESO	-63.7	0.54	-28.1	12.2	-13.9, -5.5	31.4	394.0	416.7
DSO160	-48.3	0.42	/	/	-0.2, 12.2	24.1	403.4	436.9
DSO240	-29.1	0.36	-10.86	1.2	17.2	25.5	386.5	408.7
DSO285	-22.8	0.30	-5.6	2.5	18.1	23.7	387.7	415.3

T_g glass transition temperature, T_c cold crystallization temperature, T_m melting temperature, ΔC_p heat capacity, ΔH_c heat of cold crystallization, ΔH_m heat of melting, $T_{d,10}$ % temperature at 10 % weight loss, $T_{d,max}$ temperature at maximum decomposition rate

Table 3 Curing speed and peel strength of PSA with different DSO and DSO/ESO ratios

Sample ID ^a	$m_{\text{DSO}}/m_{\text{ESO}}$ (w/w) ^b	$n_{\text{OH}}/n_{\text{Ep}}$ (mol/mol) ^c	UV passes	Peel strength (N/in.)
ESO	0	0.00	1	0.22 ± 0.04
DSO160-0.75	0.75	0.36	1	0.60 ± 0.05
DSO160-1	1	0.43	1	0.62 ± 0.11
DSO160-1.25	1.25	0.50	1	0.74 ± 0.18
DSO160-1.5	1.5	0.55	1	1.91 ± 0.12
DSO160-1.75	1.75	0.60	2	1.77 ± 0.15
DSO160-2	2	0.64	2	1.05 ± 0.08
DSO160-∞ ^d	∞	1.25	2	1.73 ± 0.13
DSO240-0.5	0.5	0.47	2	0.93 ± 0.01
DSO240-0.75	0.75	0.69	2	2.33 ± 0.24
DSO240-1	1	0.89	4	4.04 ± 0.41
DSO240-1.25	1.25	1.09	16	1.59 ± 0.31
DSO285-0.5	0.5	0.48	3	1.94 ± 0.26
DSO285-0.75	0.75	0.72	6	4.58 ± 0.81
DSO285-1	1	0.95	42	Cohesive failure

^a The designation before “-” indicates the DSO type (e.g., DSO160, DSO240, or DSO285), and the number after “-” indicates the DSO/ESO weight ratio (e.g., DSO160-0.75 means the ratio of DSO160/ESO was 0.75 in this composition)

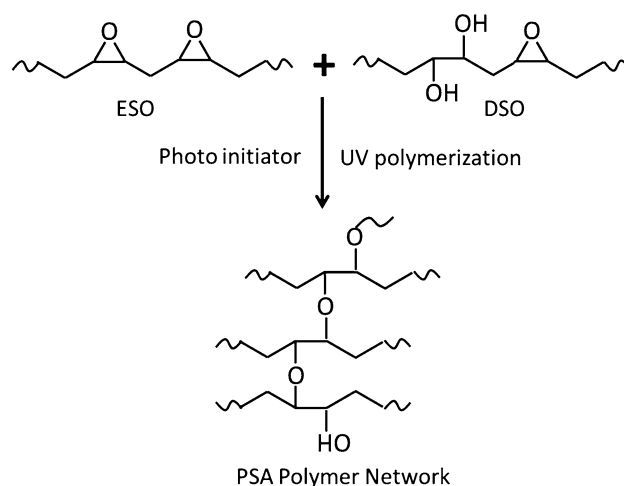
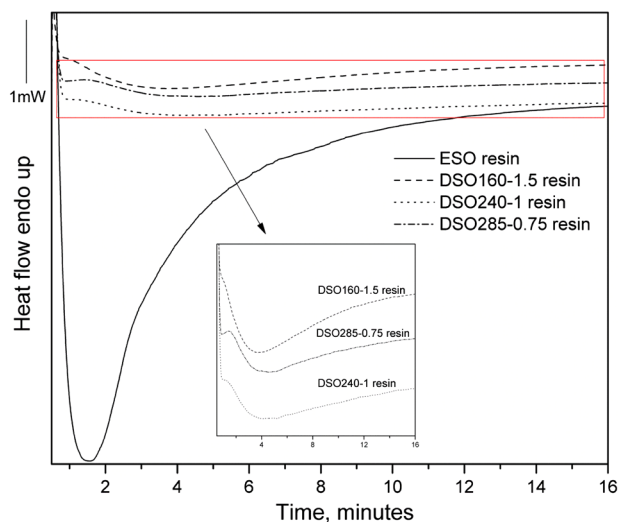
^b $m_{\text{DSO}}/m_{\text{ESO}}$ (w/w) means the weight ratio of DSO to ESO in the mixture

^c $n_{\text{OH}}/n_{\text{Ep}}$ (mol/mol) means the mole ratio of OH group to epoxy oxirane group in the mixture; n_{Ep} includes the oxirane group from both ESO and DSO

^d No ESO was added; the resin/DSO160 ratio was 0.7, and photo-initiator/DSO160 ratio was 0.03

The curing speeds of several resins (ESO, DSO160-1.5, DSO240-1, and DSO285-0.75) were further investigated using photocalorimetry (Fig. 5). The time at the peak for ESO, DSO160-1.5, DSO240-1, and DSO285-0.75 was 1.1, 3.2, 3.7, and 4.1 min, respectively, which were consistent with the UV curing passes. We also characterized the thermal properties of selected UV-cured PSAs (ESO, DSO160-1.5, DSO240-1, and DSO285-0.75) using DSC (Fig. 6). The T_g of the cured ESO was 2.92 °C, while the cured DSO160-1.5, DSO240-1, and DSO285-0.75 resins exhibited much lower T_g of −14 to −16 °C. Generally, the T_g of PSA needs to be in the range of 25–45 °C below usage temperature (e.g., room temperature), in order to possess sufficient tackiness [23].

The adhesion property of PSA was also closely related to DSO content, OHV of DSO, and $n_{\text{OH}}/n_{\text{Ep}}$ of the resin. Peel strength was measured as an indication of the PSA adhesion performance. PSA with ESO alone exhibited negligible peel strength of only 0.22 N/in. Incorporating DSO160 into ESO first increased, then decreased the peel strength. Maximum peel strength of 1.91 N/in. was obtained with a DSO160/ESO ratio of 1.5 (DSO160-1.5),

**Scheme 2** Illustration of UV-cured PSA from ESO and DSO**Fig. 5** PCA curves of PSA resins (the *squared area* is enlarged in the inserted graph so that the peaks are clearly displayed)

which corresponds to an optimal $n_{\text{OH}}/n_{\text{Ep}}$ of 0.55 in the DSO160 resins system. Because DSO160 contains both an epoxy group and a hydroxyl group, UV-curing of DSO alone without ESO also led to a considerable peel strength of 1.73 N/in., which was slightly lower than the maximal peel strength achieved for the PSA sample of DSO160-1.5. A similar trend was observed for PSA with DSO240 and DSO285, with optimal $n_{\text{OH}}/n_{\text{Ep}}$ of 0.89 for the DSO240 resin system and $n_{\text{OH}}/n_{\text{Ep}}$ of 0.72 for the DSO285 resin system. DSO240-based PSA had a maximal peel strength of 4.04 N/in., and DSO285-based PSA had a maximal peel strength of 4.58 N/in. The tackifying nature of such a PSA system was attributed to the synergistic contribution from both residue hydroxyl groups from DSO and the rosin ester. With lower $n_{\text{OH}}/n_{\text{Ep}}$ in the PSA resin, residue OH

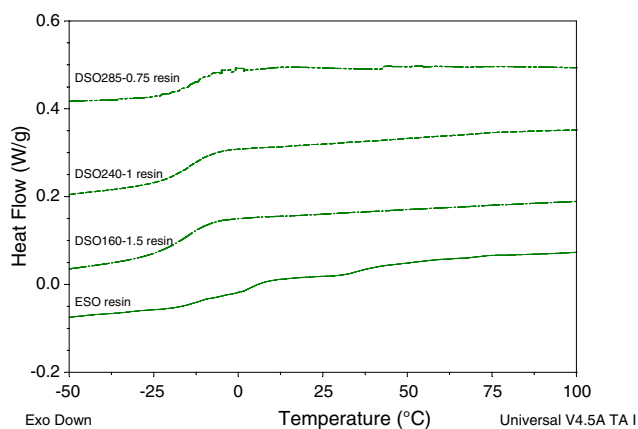


Fig. 6 DSC thermograms of selected UV-cured PSA resins

groups were insufficient for tackifying after curing. With a too-large n_{OH}/n_{EP} , curing of the resin was difficult and PSA performance was reduced. We can also conclude that higher OHV of DSO is preferred to achieve maximal adhesion.

Conclusion

DSO polyols with three different OHV were synthesized from ESO. The molecular weight and viscosity increased as DSO OHV increased. Both OHV of DSO and DSO/ESO ratio significantly affected PSA peel adhesion strength. DSO with higher OHV is preferred to achieve maximal PSA adhesion strength. The outlook for the development of plant oil-based DSO and PSA is promising due to increasing demand for versatile materials with a smaller environmental footprint, sustainability, and biodegradability. Applications of DSO polyols are not restricted to PSA but can be extended to flexible coatings and polyurethanes.

Acknowledgments The authors appreciate the funding support from Kansas Soybean Commission/United Soybean Board. Contribution No. 14-254-J from the Kansas Agricultural Experimental Station.

References

1. Johnston J (2003) Pressure sensitive adhesive tapes: A guide to their function, design, manufacture, and use. Pressure Sensitive Tape Council, Northbrook
2. Aranyi C, Gutfreud K, Hawryiewicz EJ, Wall JS (1971) Pressure-sensitive adhesive tape comprising gluten hydrolypate derivatives. US Patent 3607370
3. Cohen E, Binshtok O, Dotan A, Dodiuk H (2013) Prospective materials for biodegradable and/or biobased pressure-sensitive adhesives: a review. *J Adhes Sci Technol* 27:1998–2013

4. Bunker S, Staller C, Willenbacher N, Wool R (2003) Mini-emulsion polymerization of acrylated methyl oleate for pressure sensitive adhesives. *Int J Adhes Adhes* 23:29–38
5. Shin J, Martello M, Shrestha M, Wissinger J, Tolman W, Hillmyer M (2011) Pressure-sensitive adhesives from renewable triblock copolymers. *Macromolecules* 44:87–94
6. Ahn K, Sung J, Kim N, Kraft S, Sun X (2012) UV-curable pressure-sensitive adhesives derived from functionalized soybean oils and rosin ester. *Polym Int*. doi:10.1002/pi.4420
7. Petrovic ZS (2008) Polyurethanes from vegetable oils. *Polym Rev* 48:109–155
8. Guo A, Cho Y, Petrovic Z (2000) Structure and properties of halogenated and nonhalogenated soy-based polyols. *J Polym Sci Part A: Polym Chem* 38:3900–3910
9. Stemmelen M, Pessel F, Lapinte V, Caillol S, Habas JP, Robin JJ (2011) A fully biobased epoxy resin from vegetable oils: from the synthesis of the precursors by thiol-ene reaction to the study of the final material. *J Polym Sci Part A: Polym Chem* 49:2434–2444
10. Xia Y, Larock RC (2010) Vegetable oil-based polymeric materials: synthesis, properties, and applications. *Green Chem* 12:1893–1909
11. Desroches M, Escouvois M, Auvergne R, Caillol S, Boutevin B (2012) From vegetable oils to polyurethanes: synthetic routes to polyols and main industrial products. *Polym Rev* 52:38–79
12. Sinadinovic-Fiser S, Jankovic M, Petrovic ZS (2001) Kinetics of in situ epoxidation of soybean oil in bulk catalyzed by ion exchange resin. *J Am Oil Chem Soc* 78:725–731
13. Pfister D, Xia Y, Larock R (2011) Recent advances in vegetable oil-based polyurethanes. *Chemsuschem* 4:703–717
14. Guo Y, Hardesty J, Mannari V, Massingill J Jr (2007) Hydrolysis of epoxidized soybean oil in the presence of phosphoric acid. *J Am Oil Chem Soc* 84:929–935
15. Godoy S, Ferrao M, Gerbase A (2007) Determination of the hydroxyl value of soybean polyol by attenuated total reflectance/Fourier transform infrared spectroscopy. *J Am Oil Chem Soc* 84:503–508
16. Harry-O'kuru RE, Carriere CJ (2002) Synthesis, polyhydroxy triglycerides derived from milkweed oil. *J Agric Food Chem* 50:3214–3221
17. Lozada Z, Suppes G, Tu Y, Hsieh F (2009) Soy-based polyols from oxirane ring opening by alcoholysis reaction. *J Appl Polym Sci* 113:2552–2560
18. Lin B, Yang L, Dai H, Yi A (2008) Kinetic studies on oxirane cleavage of epoxidized soybean oil by methanol and characterization of polyols. *J Am Oil Chem Soc* 85:113–117
19. Monteavaro L, Silva E, Costa A, Samios D, Gerbase A, Petzhold C (2005) Polyurethane networks from formiated soy polyols: synthesis and mechanical characterization. *J Am Oil Chem Soc* 82:365–371
20. Ahn BK, Kraft S, Wang D, Sun XS (2011) Thermally stable, transparent, pressure-sensitive adhesives from epoxidized and dihydroxyl soybean oil. *Biomacromolecules* 12:1839–1843
21. Kong X, Liu G, Qi H, Curtis JM (2013) Preparation and characterization of high-solid polyurethane coating systems based on vegetable oil derived polyols. *Prog Org Coat* 76:1151–1160
22. Caillol S, Desroches M, Boutevin G, Loubat C, Auvergne R, Boutevin B (2012) Synthesis of new polyester polyols from epoxidized vegetable oils and biobased acids. *Eur J Lipid Sci Technol* 114:1447–1459
23. Creton C (2003) Pressure-sensitive adhesives: an introductory course. *MRS Bull* 28:434–439